



HAL
open science

Fast non-invasive monitoring of microalgal physiological stage in photobioreactors through Raman spectroscopy

Christopher Lieutaud, Ali Assaf, Olivier Gonçalves, Gaëtane Wielgosz-Collin,
Gerald Thouand

► To cite this version:

Christopher Lieutaud, Ali Assaf, Olivier Gonçalves, Gaëtane Wielgosz-Collin, Gerald Thouand. Fast non-invasive monitoring of microalgal physiological stage in photobioreactors through Raman spectroscopy. *Algal Research - Biomass, Biofuels and Bioproducts*, 2019, 42, pp.101595. 10.1016/j.algal.2019.101595 . hal-02333681

HAL Id: hal-02333681

<https://hal.science/hal-02333681>

Submitted on 25 Oct 2021

HAL is a multi-disciplinary open access archive for the deposit and dissemination of scientific research documents, whether they are published or not. The documents may come from teaching and research institutions in France or abroad, or from public or private research centers.

L'archive ouverte pluridisciplinaire **HAL**, est destinée au dépôt et à la diffusion de documents scientifiques de niveau recherche, publiés ou non, émanant des établissements d'enseignement et de recherche français ou étrangers, des laboratoires publics ou privés.



Distributed under a Creative Commons Attribution - NonCommercial 4.0 International License

Algal Research

Fast non-invasive monitoring of microalgal physiological stage in photobioreactors through Raman spectroscopy

Christopher Lieutaud ^a, Ali Assaf ^a, Olivier Gonçalves ^b, Gaëtane Wielgosz-Collin ^c, Gérald Thouand ^{a*}

^a Université de Nantes, UMR-CNRS GEPEA 6144, 18 Bd G. Defferre, 85035, La Roche sur Yon, France

^b Université de Nantes, UMR-CNRS GEPEA 6144, CRTT-BP, Bd de l'Université, 44602, Saint Nazaire, France

^c Université de Nantes, MMS EA 2160, 9 rue BIAS, BP 53508, 44035, Nantes cedex 1, France

Abstract

Microalgal bioprocesses are increasing in multiple industrial sectors for production at large scales. Nevertheless, classical sensors are still used but are not adapted for production monitoring, leading to monoparametric, invasive and time-consuming solutions. Future approaches should eliminate those weaknesses and take advantage of optical methods to optimize the monitoring. This work is focussed on the concrete application of Raman spectroscopy to characterize the physiological kinetics of a microalgal process. The monitoring of *Chlamydomonas reinhardtii* growth in photobioreactors led us to build its specific Raman spectral database. The complex Raman signatures acquired showed 35 reproducible bands for each day of growth, corresponding to the spectral fingerprints of the cell metabolites, such as chlorophyll a, beta-carotene, nucleic acids and lipids. In total, 2688 spectra were compiled in a database representing the cellular chemical fingerprints in three physiological stages and showed progressive variations between the days of acquisition. New data acquisitions allowed us to build a trial for blind validation and to characterize the bioprocesses with 89.2% accuracy. To complete the study, transcriptomic experiments following the transcript expression of two different metabolic pathways of the microalgae confirmed the cell physiology attributions made by the Raman spectroscopy. This work enables us to query the bioprocess status directly from the cells by attributing a spectrum to the current cell physiology.

*Corresponding author: Gerald.thouand@univ-nantes.fr

Keywords: Raman spectroscopy; microalgal physiology; photobioreactor; monitoring; database

1. Introduction

Microalgae are at the crossway of multiple resource productions and represent a modern solution to supply high-value-added products for the cosmetics, biofuels, health and food markets [1,2,3]. In addition to constitutive metabolites, some species of microalgae can overproduce diverse molecules of interest, such as astaxanthin, β -phycoerythrin or docosahexaenoic acid [4]. With a global market for microalgal products estimated at billions of US dollars [5,6], cultures of microalgae for industrial use have been developed at large scale and consist of either open ponds, up to hundreds of hectares, or closed photobioreactors, up to 700 m³ [7]. The microalgal production sites are generally estimated in megaton per hectare per year, and some cultures could last for months, depending on the strain used [8,9].

Classical approaches are currently applied to monitor these large-scale productions, and only classical analytical methods are used [10]. The algal cell physiology is followed through time with phenotypic observations (size, shape, colour) and monoparametric disposable probes (pH, temperature, biomass, pCO₂, pO₂) placed into the reactors [11]. The microalgal production is then indirectly estimated by correlating the physico-chemical environment with the cell physiology. This overall monitoring implies the need to have as many classical sensors as pieces of information desired, but numerous parameters are needed to follow this highly dynamic bioreaction [12,13]. The large number of sensors needed being difficult to pursue for industrial purposes, the cells should be focussed instead on directly collecting information for bioprocess monitoring [14]. Ideally, the monitoring should involve the minimum number of sensors with the maximum of information, increasing the understanding of the system, decreasing the bioprocess cost, and leading to more competitive microalgal bioproduction. To improve the bioproduction control, the characterization and quantification of the cell components can be assured by multiparametric methods such as chromatography and mass spectrometry [15]. Despite their high sensitivity and specificity, these methods need repeated sampling for bioprocess control and lead to time-consuming analysis that can

be done by only qualified operators confined in a lab. At the process scale, their utilization results in a global decrease of the harvest and an increased exposure to contamination by multiple sampling [16]. Nuclear magnetic resonance has also been well investigated for monitoring biomass and metabolites, but it needs much time and a high cell density for analysis, as well as a reactor setup in a magnetic chamber [16]. Technological developments in the last few years have adapted optical methods for integration in situ, each one having advantages and inconveniences [17,18]. UV-visible spectroscopy offers a low-cost and quick spectral representation of a bioprocess monitoring but has a low specificity to cellular compounds [10]. Another solution is fluorescence spectroscopy, providing in situ measurements, but its use is specific to fluorescence-active compounds [10]. Infrared spectroscopy has also been studied, as it enables rich spectral signatures of a sample, but its application is limited by the high absorbance of water molecules [10]. Optical methods are generally already well established in the pharmaceutical area, monitoring substrates produced from microorganisms such as yeast and bacteria (carotenoids, lactate, phenylalanine), but they do not focus on the cell itself [19,20]. A time gap is present between the moment of metabolites productions by the cells and their measurements by analytical methods so focusing on the cells should improve the monitoring. Distinct from other optical methods, Raman spectroscopy affords the possibility to directly study cells in a medium and to discriminate between microalgal species or stress status by acquiring Raman spectral fingerprints [21,22]. The main feature of Raman spectroscopy is non-invasive measurements, in a few seconds, of entire cells without metabolite extraction or addition of reactive [23,24]. This multiparametric methodology has been identified as a candidate for future bioprocess monitoring tools [24]. This technique is based on the inelastic scattering of a monochromatic light interacting with a sample. This interaction leads to the spectral fingerprint of the sample composition. The bioproducts synthesized by microalgae in response to a stress have specific chemical bonds corresponding to specific Raman bands [25,26,27]. For lipid production, the single presence and position of an unsaturation may change the Raman spectrum and enable the discrimination between different lipids

[28,29,30]. The triacylglycerol and starch production of specific species has also been investigated [31,32]. From the perspective of a bioprocess, the multiparametric, fast, and non-invasive analysis of a bioreaction should have improved efficiency by monitoring cells directly and complementing the classical sensors. Currently, however, the correlation between Raman spectra and the physiology of microalgae has been poorly investigated in such monitoring. Out of all the studies published on Raman spectroscopy, no method is available, to our knowledge, to demonstrate the physiological stage monitoring of homogeneous populations of microalgae from photobioreactors. The dynamic physiology of microalgae has been the focus of fundamental research at low scales and over short periods (1 day) in stress conditions [33]. One study presented an approach to monitor diatom growth in an unstirred flask by Raman spectroscopy and showed spectra fluctuating through time [34]. That study allowed correlations between cell physiology and Raman fingerprints, but applications and proof of concept for monitoring an entire bioprocess from spectral fingerprints have yet to be demonstrated. A robust spectral database acquired offline could indeed be the source of quick and complete culture characterizations. The work presented on this paper focusses on concrete application of Raman spectroscopy for predicting the physiological stage of a microalgal population with single-blinded trial correlations carried out on *Chlamydomonas reinhardtii* growth in photobioreactors. The recent decades of research on microalgal metabolism have led to a better understanding of the genomic [35,36], metabolomic [37,38] and lipidomic levels [39,40]. The kinetics of microalgal physiology has even been well described for a few species through complex analyses, such as metabolomics carried out on *Chlamydomonas reinhardtii* [41]. The microalga *Chlamydomonas reinhardtii* was selected for our experiments based on its well-studied physiology [42]. The quantifications of transcripts associated with the lipid metabolic pathways (146945) and with tubby-like proteins production (26047) enabled *Chlamydomonas reinhardtii* physiological stage discrimination. Unlike usual approaches made by Raman spectroscopy, the observations made by our method are validated with referential transcriptomic experiments to confirm the correct correlation to the cell physiology. This first

work is a prerequisite that could lead to predictions on other applications such as metabolites productions and online monitoring.

2. Materials and methods

2.1. Microalgal strains and culture conditions

Chlamydomonas reinhardtii wild-type strain (137 AH) was supplied from the CEA Cadarache (France). The axenic strain was cultivated in Sueoka autotrophic medium. The medium was composed as follows for 960 mL of solution: NH₄Cl 1.45 g (Merck, ref 1.01145); MgSO₄·7H₂O 0.28 g (Sigma-Aldrich, ref 63138); CaCl₂·2H₂O 0.05 g (Merck, ref 1.02382); KH₂PO₄ 0.61 g (Sigma-Aldrich, ref 795496) and 1 mL of Hutner's trace elements solution [43,44]. The medium was autoclaved at 121°C for 21 minutes. A solution of NaHCO₃ 1.68 g (Merck, ref 1.06329) in 40 mL was filtered separately with 0.2-µm filters and added to fill the medium to one litre. Preculture growth was sustained at 130 rpm and 25°C under continuous light (incident photon flux density of 30 µmol·m⁻²·s⁻¹) in an incubator (Eppendorf, New Brunswick Innova 42r). Two-hundred-millilitre *Chlamydomonas reinhardtii* precultures were carried out in 500 mL Erlenmeyer flask for 21 days until use in photobioreactors.

Cultivations in photobioreactors were conducted in batch mode. Experiments were carried out in airlift photobioreactors with a working volume of one litre and a specific illuminated surface area (alight) of 33.3 m⁻¹. The photobioreactor dimensions are 21 x 35 x 4 cm. The photobioreactor setup is described in previous publications [43,45]. The photobioreactors' front panels were made of methyl methacrylate, and the rear sides were stainless steel (type 316L). Photobioreactors were illuminated under continuous light (incident photon flux density of 120 µmol·m⁻²·s⁻¹) by a panel of LEDs (Bionef, Z1 panel, France). A probe continuously measured both pH and temperature (Mettler Toledo, 4801i). A cryothermostat (Lauda, RC20) fixed the temperature at 25°C (± 0.1°C) through cooling tubes on the rear side of the photobioreactor. The pH was fixed at 7.5 and was controlled by injecting CO₂ through solenoids coupled with a transmitter (Mettler Toledo, M300) (figure 1). The inoculation of photobioreactors was fixed at optical density (O.D.) = 0.1 at 750 nm.

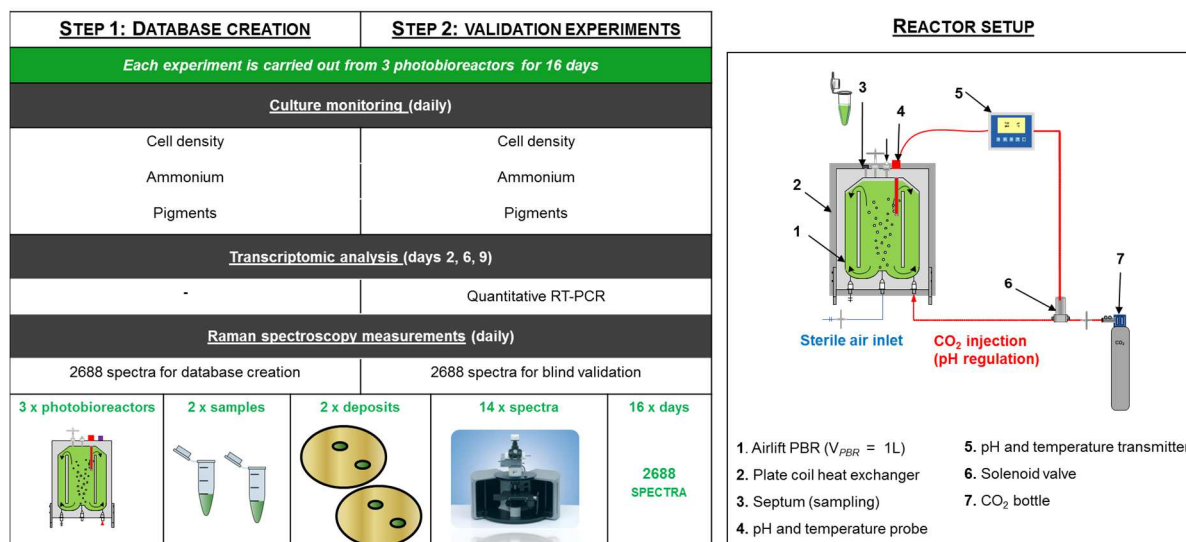


Fig. 1.(colour) Diagram of analyses done and the schema of *Chlamydomonas reinhardtii* batches in photobioreactors. The experimental plan is subdivided in two steps: creation and blind validation experiments.

Experiments in two steps were carried out. The first one was a database creation in order to collect the Raman spectra of *Chlamydomonas reinhardtii* growth for each day and make a model. The second step is a validation experiments setup made to test blind predictions.

2.2. Culture monitoring

A set of methods was applied daily to follow the growth of *Chlamydomonas reinhardtii* for 16 days. The cell estimations were carried out by monitoring the optical density at 750 nm from 1 mL of sample with a spectrophotometer (BMG Labtech, SPECTROstar^{Nano}, v2.11). The cell density was also determined under an optical microscope using Malassez counting cell and was expressed in cells per milliliter of culture. Ammonium concentration was monitored by colorimetric reactions using a Hach Lange kit LCK303, based on the ISO 7150-1 standard [44, 46]. Ammonium was measured by a spectrophotometer (Hach, DR 2800).

Finally, chlorophyll a and beta-carotene concentrations were monitored after extraction. Extractions were performed from 1 mL of microalgal sample with methanol [47]. The extraction was done by incubation at 44°C for 30 minutes, followed by centrifugation at 12,200 g for 5 minutes. The absorption was measured in quartz cuvettes at 480, 652, 665

and 750 nm, from which the concentrations of beta-carotene and chlorophyll a were calculated [48].

2.3. Transcriptomic analysis

Three samples were harvested from different days of growth (2, 6 and 9) to confirm the physiological stage of *Chlamydomonas reinhardtii*. RNA was extracted by grinding Whatman filter paper GF/F into powder with liquid nitrogen. An RNA extraction kit (Macherey Nagel, NucleoSpin RNA plant) was used to purify RNA. Afterward, cDNA was retrotranscribed and amplified (Promega, GoTaq). Measurements of qPCR were realized with a StepOnePlus Real-Time PCR-System (ThermoFisher, v2.1). Oligonucleotides and protocols were reproduced from a previous work done by Lv & al [42]. Data were normalized according to the *Rack1* transcript quantification, used as a constitutive control gene and linked to the scaffolding protein receptor for activated C kinase 1. Transcriptomic analyses were done in the laboratory of MMS, Le Mans, France.

2.4. Raman spectroscopy measurements

The Raman spectra were acquired using a Raman microspectrometer (Bruker Optics, Senterra, Germany) driven by Opus software (Bruker Optics, v7.2). This device was equipped with a CCD camera cooled at -60°C and a BX51 Olympus microscope. The grating (400 lines/mm) and the objective LMPlanFLN100x/0.8 were used for these experiments. The analyses were performed offline at 785 nm with a laser power of 10 mW on the sample. The spectral resolution was approximately 8 cm⁻¹. Three acquisitions of 10 seconds each were done for each spectrum. The parameters used were tested to ensure that irradiance didn't affect the cells [49]. The Raman spectra were acquired in two steps. A first step consisted in a database creation, including 2688 Raman spectra from daily measurements in three photobioreactors for 16 days of culture. Then, a second step consisted in blind validation experiments and was also carried out with 2688 spectra (figure 1). No discard was proceeded on the spectra to be tested as close as possible to real applications. Daily, two

samples of 2 mL of microalgae were harvested from each photobioreactor and centrifuged at 8000 g for 10 minutes, and 2 deposits of 2 μ L from the pellets obtained were spread onto gold surfaces (Bio-logic Science Instruments, France, ref SE-9AU-M). The sample measurements on gold surfaces are adapted from a previous work [50]. A total of 14 spectra were acquired for each deposit (3 replicates x 1 photobioreactor x 16 days x 2 samples x 2 deposits x 14 spectra = 2688 spectra for each step).

2.5. Pre-processing spectra and data analysis

Raman spectra were first processed using Opus software. No spectrum was discarded; a simple visual checkup was done to ensure no cosmic ray was occurring. The pre-processing steps were applied on all spectra independently for statistical comparison. The Raman spectra were acquired with a Raman shift range from 300 to 3200 cm^{-1} and were cut between 300 and 1800 cm^{-1} . The spectra were pre-processed by an elastic concave baseline correction (64°; 10 iterations). Data were normalized using maximum-minimum bands to normalize each spectrum independently. The carotenoid band at 1523 cm^{-1} was the highest signal and was used for normalization. To improve the model recognition in physiological stages, a probabilistic quotient normalization (PQN) was applied with MATLAB software, using the statistics toolbox (MathWorks, Inc. vR2012b, France) completed by the SAISIR package [51]. PQN calculates the median of quotients of each X point on spectra to the median point then corrects X. PQN intends to reduce unwanted biases [52]. To optimize the discrimination of the database, the spectra were normalized by PQN in 16 groups, corresponding to the 16 days of growth. MATLAB software was also used for multivariate data analyses. First, the study was focussed on the physiological stage characterization by building a database of 2688 Raman spectra. Principal component analysis (PCA) was applied for data exploration in the database by using the first three components. A factorial discriminant analysis (FDA) was used in parallel, with the “fda2” function, as a supervised method to evaluate the spectral data repartition from the three physiological stages, using the first five PCA scores and the average of 100-fold iterations. The inter-batch

reproducibility of the Raman spectral database was analyzed with an average correlation coefficient of 94% for each day of growth. The Kruskal-Wallis test was applied to the database, using the “Kruskal-Wallis” function, to analyse the data distribution in the 16 groups corresponding to the 16 days of growth ($p=0.05$). Then, in a second independent effort, the experiment was focussed on the blind validation of the database by matching a maximal number of random Raman spectra against the database with the acquisition of a new data set of 2688 Raman spectra. By FDA, the 2688 spectra from the step 2 (validations experiments) were matched one by one against the complete database from step 1 and attributed to a stage (exponential, deceleration, stationary). This validation corresponded to a single blind trial and was carried out through FDA using the function “*applyfda1*”, based on the first five PCA scores-

3. Results and discussion

3.1. Matching the microalgal physiological stages by Raman spectroscopy

The culture growth of *Chlamydomonas reinhardtii* cells in the photobioreactors was monitored by optical density at 750 nm and ammonium measurements (figure 2.A). As expected, the culture's growth was separated into three different physiological stages. The optical density measurements showed three different phases. The optical density from day 0 at 0.1 log (± 0.01) to day 2 at 1.5 log (± 0.3) determined the exponential stage. A second phase is observed from day 3 at 4.7 log (± 1.3) to day 7 at 15.3 log (± 0.8) as the increase of the optical density slow down and characterized the deceleration stage. Finally, the stationary stage was indicated by the global stabilization of the optical density at 15.6 log (± 0.6) after day 8. Ammonium measurements showed a complementary behaviour during the growth, with a strong decrease between the exponential and deceleration stages, starting on day 0 at 605 mg·L⁻¹ (± 4.6) and slowing to 158 mg·L⁻¹ (± 16.1) at day 7. The stabilization of ammonium measurements after day 8 at 147 mg·L⁻¹ (± 7.3) helped identify the stationary stage and the presumed threshold of limited light transmission through the stagnation of metabolism [53]. Optical density and ammonium measurements were done with three photobioreactors and both led to R² of 0.99. The offline monitoring setup included, in parallel, daily measurements of pigment concentrations to control the general state of the culture, showing global increases in chlorophyll a and beta-carotene, from, respectively, 0.41 µg·mL⁻¹ (± 0.1) and 0.15 µg·mL⁻¹ (± 0.03) on day 0 to 16.91 µg·mL⁻¹ (± 0.6) and 5.56 µg·mL⁻¹ (± 0.06) on day 15 (figure 2.B). This increase follows partially the increasing cell density through the growth. The carotenoid-chlorophyll a ratios showed thin pigments variations through the growth with a decrease from 1.24 to 0.88 on the exponential stage, followed by a progressive stabilization towards 0.94 on the day 15, confirming the absence of nutrient limitation as no significant variation are observed (fig SD1) [54,55].

Alongside these daily analyses, the spectral database creation was carried out. Raman spectroscopy was applied to acquire the evolution of the Raman spectral fingerprints through

the growth of *Chlamydomonas reinhardtii*. Averaged Raman spectra were associated with each physiological stage and are represented in figure 2.C. Thirty-five Raman bands were present on the spectra, with a coefficient of variation under 0.3, and were considered reproducible [56]. Those 35 bands were selected for the analysis and were attributed to usual chemical molecules from microalgae [57,58,59]. The main Raman bands represented (medium and high signals) were attributed to pigment signals, with a strong Raman response, according to characteristic bonds vibrations, deformations and stretching. Beta-carotene signals were associated with Raman bands at 1150 cm^{-1} ($\delta(\text{C-C})$, $\delta(\text{C-H})$), 1390 cm^{-1} ($\delta(\text{C-H}_3)$), and 1523 cm^{-1} $\nu(\text{C=C})$ and chlorophyll a with bands at 744 cm^{-1} ($\delta(\text{H-C-O})$, $\delta(\text{N-C-C})$), 915 cm^{-1} ($\delta(\text{N-C-C})$ $\delta(\text{C-C-C})$), 988 cm^{-1} ($\delta(\text{C-H}_3)$), 1186 cm^{-1} ($\delta(\text{C-H})$, $\nu(\text{N-C})$), 1325 cm^{-1} ($\nu(\text{C-N})$, $\delta(\text{C-H})$) and 1390 cm^{-1} ($\delta(\text{C-H}_3)$, $\delta(\text{C-H})$, $\nu(\text{C-N})$) (figure 3.D) [22,57,58]. These Raman bands were present on the spectra of each day of growth. From the overall Raman spectra, the signals increased during the growth, enabling us to distinguish the Raman fingerprints into three different stages. The beta-carotene and chlorophyll a concentrations increased through the growth alongside cell density. Their Raman band intensities of beta-carotene and chlorophyll a rose by a factor 1.3 (± 0.3) between the exponential and deceleration stages and reached a factor 1.8 (± 0.6) and 1.5 (± 0.4), respectively, between the exponential and stationary stages. Pigment intensities from Raman spectroscopy through growth were well correlated with their chemical dosage, resulting in an R^2 of 0.83 for beta-carotene and 0.85 for chlorophyll a (figure SD.2). Other signatures, such as carbohydrates, were present on the spectra with a weaker Raman signal response, such as α -D-glucosides at 479 cm^{-1} ($\delta(\text{C-C-C})$), polysaccharides at 517 cm^{-1} ($\delta(\text{CH}_2)$, $\delta(\text{C-OH})$) or 744 cm^{-1} ($\nu(\text{H-CO})$), and calcium alginate at 1435 cm^{-1} , through symmetric COO^- stretching [28,58]. Nucleic acids were also present on the spectra with medium Raman bands between 600 and 800 cm^{-1} , corresponding to ring breathing vibrations, and at 1100 cm^{-1} through symmetric PO_2 stretching vibrations [58,59]. On other part of the spectra, amino acid signatures have been associated with Raman bands, such as leucine at 1186 cm^{-1} or L-tryptophan at 870 and 1486 cm^{-1} or hydroxyproline by a shoulder at 850 and 875 cm^{-1}

[59,60,61]. Other intermediate signatures can be associated with adhesion proteins, such as amide I at 1656 cm^{-1} and amide III at 1223 cm^{-1} [28,58]. With even weaker but still prominent signatures, lipid molecules can be identified at 1656 cm^{-1} due to cis C=C stretching and at 1750 cm^{-1} through C=O vibrations [31]. The Raman bands presented in the exponential stage were still observable in the deceleration and stationary stages, enabling us to analyse the spectral database.

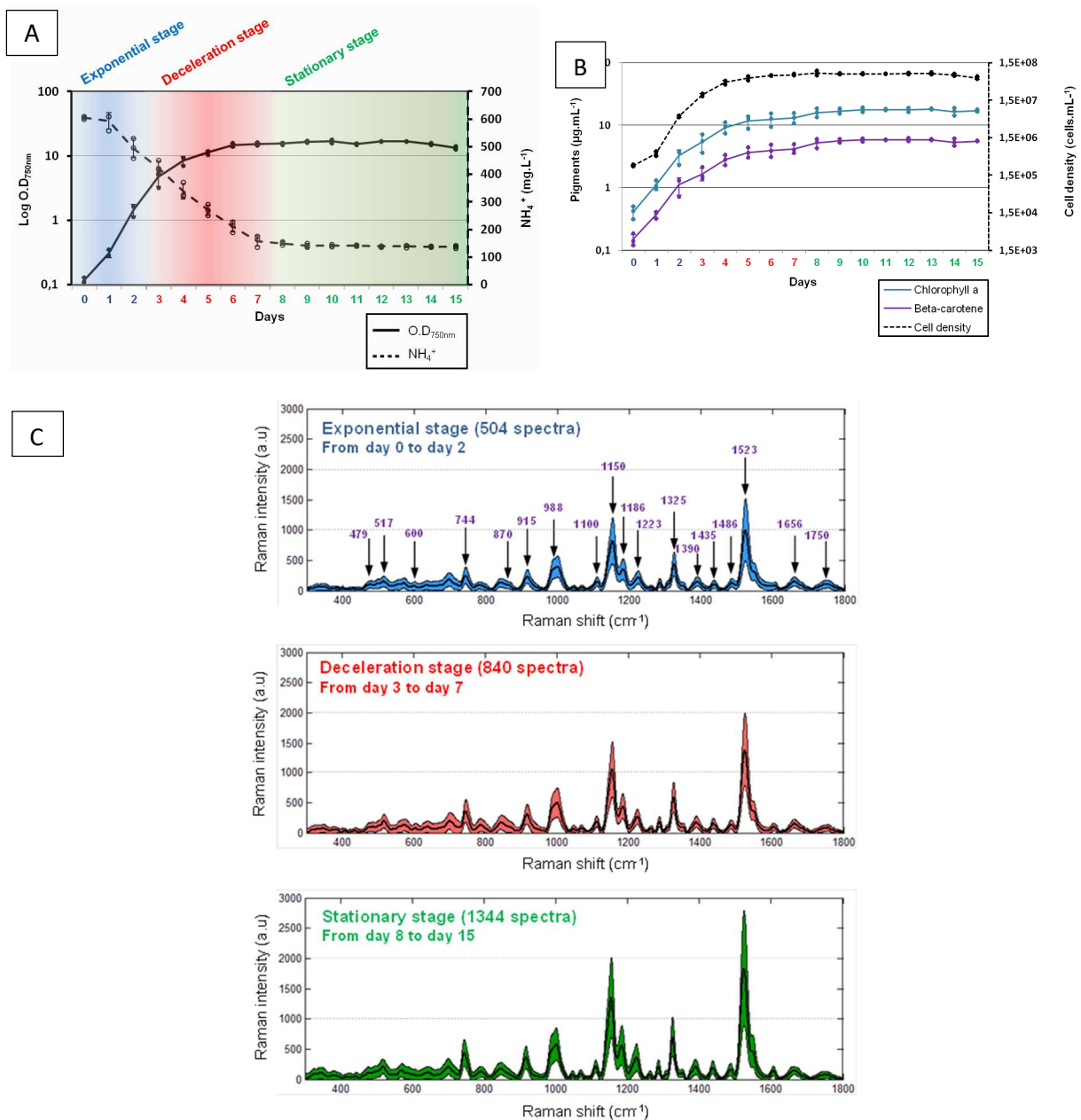


Fig. 2.(colour) A. Monitoring of *Chlamydomonas reinhardtii* in Sueoka medium in photobioreactors from day 0 to day 15 (n=3). **B.** Chlorophyll a and beta-carotene concentrations increasing with the cell density throughout the growth of *Chlamydomonas reinhardtii* in a photobioreactor (n=3). **C.** Average raw Raman spectra acquired for the exponential, deceleration and stationary stages, represented in a full line. The standard deviations are represented in shades around the spectra. Raman bands with strong and medium signatures are represented by arrows.

3.2 Raman spectral database exploration

Multivariate statistical analyses were carried out to visualize the Raman spectra repartition and identify the bands from the spectra influencing the separation into three physiological stages. The distribution of the total 2688 Raman spectra included in the database was first analysed by PCA, leading to a representation with the three main components that showed spectra being distributed according to their days of acquisition towards the left (figure 3.A). Depending on the day of acquisition, the Raman spectra were clustered into three different groups. The spectra from the two extreme stages were well separated, with the exponential stage at the utmost right and the stationary stage at the opposite. On the other hand, the deceleration stage overlapped them in the centre of the representation, as expected, and thus made the separation into stages more difficult. The three main components displayed in the PCA explained 39.5% of the information and represented the loadings responsible for the separation observed between stages, including variance shifts between -0.1 and 0.1 (figure 3.B). The signals above 0.025 were selected as Raman bands contributing the most to the shifts between physiological stages and are detailed in figure 3.D. The first loading (L1) represented the main component, with 24.4% of the information, and represented the lateral distribution on the PCA representation. It included a preeminent signal at 1523 cm^{-1} attributed to carotenoids, which increased with time. The second loading (L2) represented 10.3% of the information and displayed multiple signatures above 0.025 with Raman bands from pigments, well represented at 1523 and 1150 cm^{-1} (carotenoids) and at 988 and 1325 cm^{-1} (chlorophyll a). Other Raman bands were present at 744 cm^{-1} with a mixed contribution from both chlorophyll a and carbohydrates and at 1186 cm^{-1} with mixed signals from chlorophyll a and amino acids. Weaker signals also contributed to the separation between stages through polysaccharides at 517 cm^{-1} , nucleic acids between 600 and 800 cm^{-1} , and finally lipids at 1656 and 1750 cm^{-1} . The third main loading (L3) represented only 4.8% of the information and indicated the contribution of Raman response bands from carotenoids at 1523 cm^{-1} , chlorophyll a at 988, 1186 and 1325 cm^{-1} , carbohydrates at 1186 cm^{-1} , and nucleic acid

signatures between 600 and 800 cm^{-1} . The weakest Raman bands presented in figure 2.C were also present on the loadings L2 and L3 but made a lesser contribution to the physiological stage separation (signals under 0.025). The most contributing bands for stage discrimination are attributed to polysaccharides, ribonucleic acids, carbohydrates, chlorophyll a, carotenoid, amide I, amino acids and lipids. The eleven main Raman bands identified on the three loadings indicated kinetic switches of metabolites during the growth batch as having key roles in separating the spectral fingerprints for each physiological stage. Metabolomics studies have also established pigments, amino acids, and lipids as key metabolites for physiological shifts during *Chlamydomonas reinhardtii* batch growth [41].

To interpret the Raman signature switches during growth, loading 2, including most of the signals, was analysed separately over time with the Kruskal-Wallis test (figure 3.C). The analysis showed in detail, once again, the spectra from the exponential and stationary stages separated well, but the extreme days of the deceleration stage overlapped the other two stages, indicating the non-synchronous growth of cells (days 3 and 7). Other studies made on Raman spectroscopy of microalgae observed the same trends, without including the days between the stages in the database [34]. The spectral fingerprints obtained by the statistical model nevertheless confirm trends of separation between the day of acquisition and each physiological stage. This database is considered as our model for carrying out blind predictions.

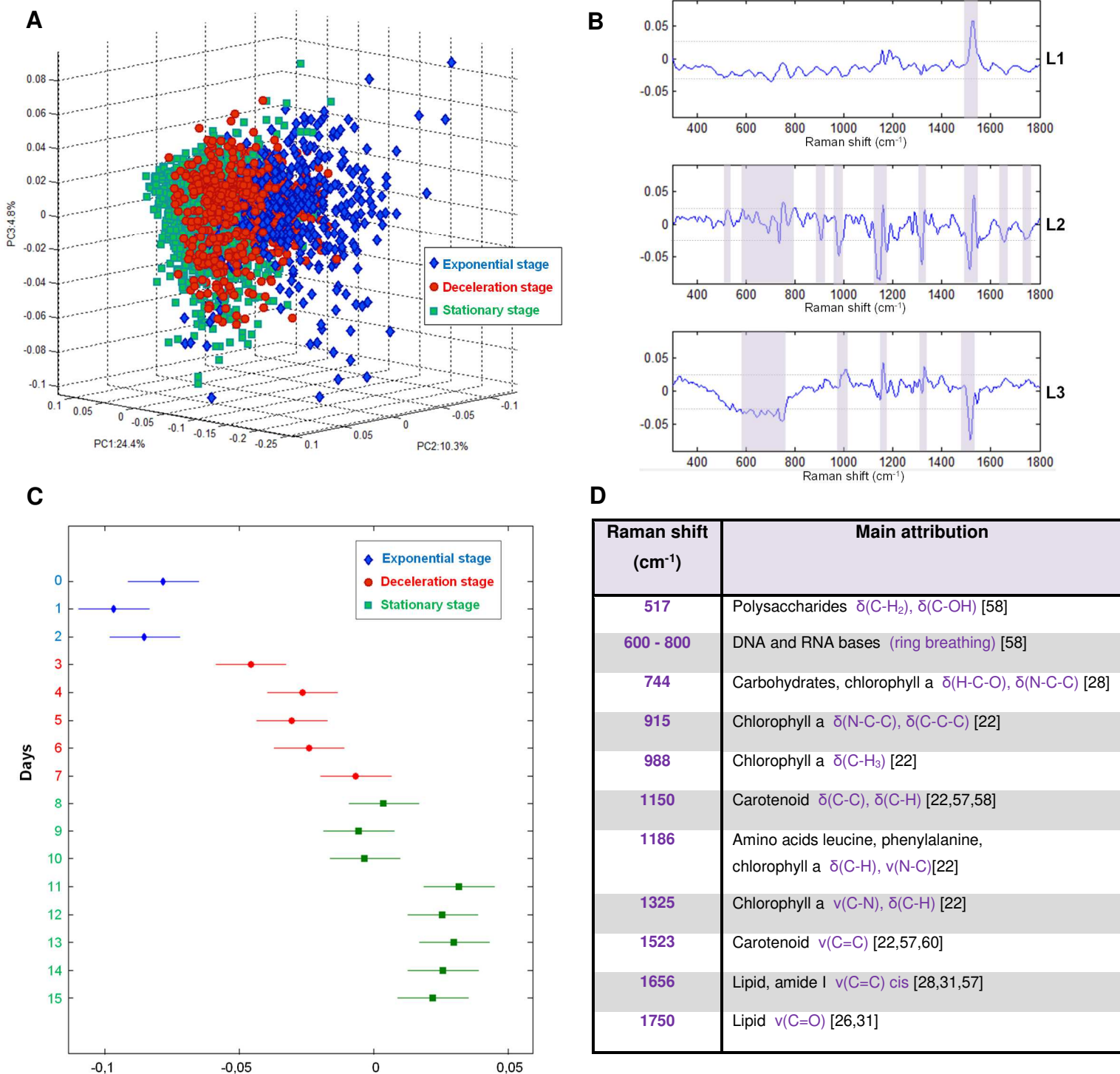


Fig. 3.(colour) A. Three-dimensional representation of principal component analysis (PCA) from the 2688 Raman spectra included in the spectral database (PC1 24.4%; PC2 10.3%; PC3 4.8%). **B.** Three main PCA loadings. Raman bands responsible for stage discrimination are highlighted. **C.** Kruskal-Wallis test, based on loading 2, with the most bands, depicting the variance of the 2688 spectra over time. **D.** Attribution of Raman band loadings (ν for stretches; δ for deformation).

*3.3 Prediction of the physiological stage of *Chlamydomonas reinhardtii**

To test our model, discriminant analyses were applied to a new Raman data set. This experiment intended to confront the loadings identified by PCA to the concrete application of attributing an unknown Raman spectrum to its correct cell physiological stage. FDA was applied as a single blind test to 2688 Raman spectra from new photobioreactors against the already compiled database. The spectra acquired from days close to stage transitions were included in the model to ensure the most concrete approach by studying the complete bioprocess dynamic behaviour. Previous studies adopted the other approach, including the spectral borderlines, to optimize the physiological stages interpretation by improving the model stability [34]. The FDA showed that the Raman spectra acquired between days 0 and 2 was well recognized as coming from an exponential stage (figure 4.A) and highlight the stage recognition for the first two days, with up to 96% of correct attribution. This highest discrimination was in the middle of the stage in (day 1), and day 0 presented 85% of correct attribution. Attributions to the exponential stage strongly decreased after day 2, with 36% wrong attribution from day 2 to the deceleration stage (figure 4.B). Raman spectra acquired between days 3 and 7 were correctly attributed to the deceleration stage with more than 76% correct attribution. The Raman spectra falsely attributed to the deceleration stage were acquired from days 2 and 8, the closest days to the deceleration stage. Regarding the attributions of Raman spectra to the stationary stage, a slow increase in recognition was seen after day 2 and showed a sudden and strong increase in correct attribution (from 77% to 100%) to the stationary stage after day 8 (figure 4.C). The overall distribution of Raman spectra was, as expected, well separated into the three stages. The middle days of each stage (days 1, 4-6, and 9-15, respectively) were highly discriminatory, with a correct attribution above 80%. Nevertheless, the attribution for days between stages was lower than the average, with a prediction under 65% for day 2 and 80% for days 7 and 8. Raman spectrum attributions for these days also presented the highest standard deviation. This phenomenon confirms the observation from figure 3.C supporting the asynchronous

physiology of cells during growth, some cells shifting to the next physiological stage earlier than others [62].

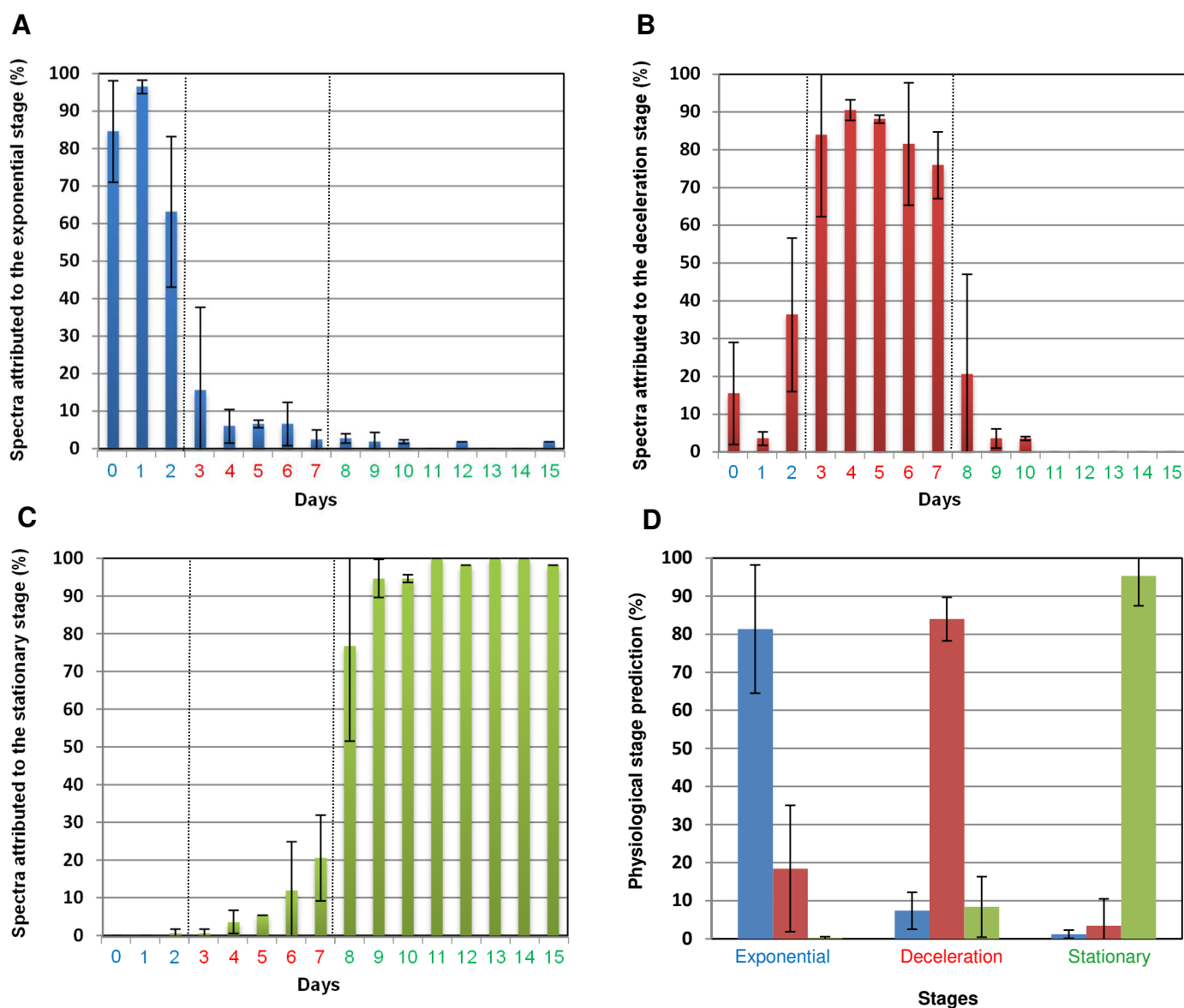


Fig. 4. (colour) A. B. C. Blind validation of 2688 Raman spectra by factorial discriminant analysis against the exponential, deceleration and stationary stages of the spectral database of *Chlamydomonas reinhardtii* growth. **D.** Global prediction of the Raman validation of the three stages. The exponential, deceleration and stationary stages are, respectively, depicted in blue, red and green.

The capacity of this analysis to predict correctly the physiological stage is summarized in figure 4.D. The detailed predictions made indicate a trustworthy method, showing strong attribution of spectra in the correct physiological stage and few false positives, mostly for days close to the correct stage. On average, the exponential stage was well predicted at 81.4%, the deceleration stage at 84%, and the stationary stage at 95.3%. For the whole 16 days, the average prediction rate was 89.2%. This prediction rate can be related to similar work done on other cellular models. Discriminant analysis made on *Lactobacillus* describes, for example, a correct prediction of 91% over 30 hours of growth [63].

3.4 Transcriptomic validation of the Raman spectroscopy method

Physiological studies made on *Chlamydomonas reinhardtii* report that specific transcripts fluctuate in expression through the growth and physiological stages [42]. Other studies made on microalgae have highlighted the qRT-PCR for physiological state validation as a robust methodology [64]. Analyses by qRT-PCR were carried out to confirm the cell attributions in the three physiological stages in photobioreactors. Samples of cells from days 2, 6 and 9 were harvested and analysed, each group representing a physiological stage (figure 5). The quantification of transcript 146945, corresponding to the gene G3DPH, is depicted in figure 5.A. Its expression level increased, with a ratio of 4.5 between the exponential and deceleration stages and a ratio of 17.7 between the exponential and stationary stages. This transcript is indirectly correlated to lipid metabolic pathways linked to neutral lipid accumulation during the stationary phase and is reported to increase over time [42,65]. As a contrasting example, the quantification of the transcript 26047, correlated to tubby-like protein production, is shown in figure 5.B. The ratio of its expression decreased to 4.3 between the exponential and deceleration stages and a ratio of 26 between the exponential and the stationary stages. This transcript is also well known to decrease with time [42]. The quantification of both transcripts confirmed the expected kinetics of microalgal physiology in our photobioreactors and validated the Raman-spectral interpretation, separating spectra into three distinct physiological stages.

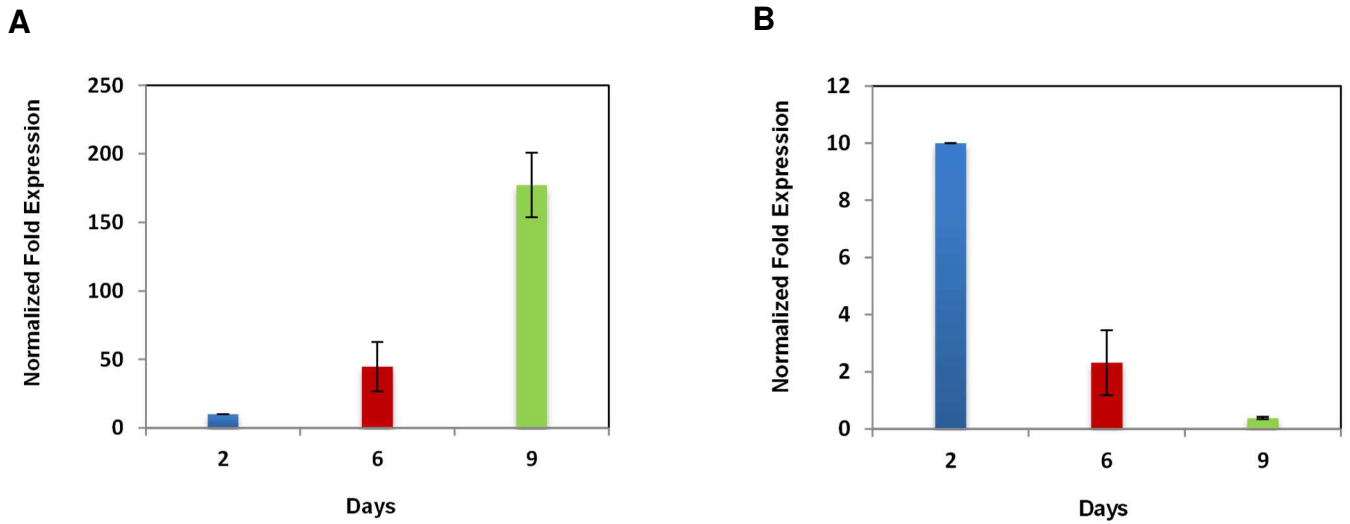


Fig. 5. (colour) Expression of two transcripts related to *Chlamydomonas reinhardtii* physiology, as determined by qRT-PCR, normalized to the expression of *Rack1* as the internal control. The two transcript expression levels were set at 10 for the exponential stage. **A.** Quantification of transcript 146945, associated with the gene G3DPH. **B.** Quantification of transcript 26047, associated with tubby-like proteins.

4. Conclusion

Raman spectroscopy offers a good alternative for future prospects on fast acquisitions and non-invasive physiological stage monitoring for bioprocess cultures. Its multiparametric advantages over classical methods lead to a clear observation of all compounds in the sample in a few seconds. By making a robust database, this method enables researchers to monitor the good conduct of a reactor. Unlike other approaches, the method presented in this paper enables us to query the bioprocess state directly from the cell by giving an instant prediction of the current physiological stage. The desynchronization and resynchronization of cells between physiological stages is also estimable with this method. The predictions obtained presented an average accuracy of 89.2% for correct attribution in the three physiological stages combined. This method could be improved by increasing the spectral database size and could lead to discrimination with the same accuracy into more than three stages. For future developments, the automatization of the spectral fingerprint database for continuous monitoring and the implementation of a Raman probe inside photobioreactors for online monitoring should be direct improvements of the method, making it closer to a final system for industrial monitoring.

Acknowledgements

This research has been supported by the University of Nantes. The authors thank H el ene Marec for technical assistance on photobioreactor setup and Rapha elle Touchard for microalgal strain support. Transcriptomic experiments were done in collaboration with the MMS team of Le Mans (France), and we acknowledge Pr Nathalie Casse, Dr Aurore Caruso and Marie Zanella for the help in qRT-PCR experiments.

Author's contributions

Christopher Lieutaud, Ali Assaf, Olivier Gonçalves, Gaëtane Wielgosz-Collin and Gerald Thouand have participated in the conception and the design of the study.

Christopher Lieutaud and Ali Assaf have conducted the experiments.

Christopher Lieutaud, Ali Assaf and Gerald Thouand have analyzed and interpreted the data and drafted the manuscript.

Ali Assaf, Olivier Gonçalves, Gaëtane Wielgosz-Collin and Gerald Thouand supervised the research.

Christopher Lieutaud, Ali Assaf, Olivier Gonçalves, Gaëtane Wielgosz-Collin and Gerald Thouand have critically reviewed the manuscript. All authors agree to authorship and the submission of this manuscript.

I hereby Gerald Thouand, certify to be responsible of this work in its integrity.

Gérald THOUAND
Gerald.thouand@univ-nantes.fr



La Roche sur Yon, 14/05/2019

Declaration of interest

There is no conflict of interest declared for any of the authors of this manuscript. No conflicts, informed consent, human or animal rights applicable.

References

- [1] Y. Tang, J. N. Rosenberg, P. Bohutskyi, G. Yu, M. J. Betenbaugh, F. Wang, **Microalgae as a feedstock for biofuel precursors and value-added products: Green fuels and golden opportunities**, *Bioresources*, 11 (2016), pp. 2850-2885.
- [2] D. Gangl, J. A. Z. Zedler, P. D. Rajakumar, E. M. R. Martinez, A. Riseley, A. Włodarczyk, S. Purton, Y. Sakuragi, C. J. Howe, P. E. Jensen, C. Robinson, **Biotechnological exploitation of microalgae**, *J. Exp. Bot.*, 66 (2015), pp. 6975–6990.
- [3] M. Rizwan, G. Mujtaba, S. A. Memon, K. Lee, N. Rashid, **Exploring the potential of microalgae for new biotechnology applications and beyond: A review**, *Renew. Sustain. Energy Rev.*, 92 (2018), pp. 394–404.
- [4] G. Markou, E. Nerantzis, **Microalgae for high-value compounds and biofuels production: a review with focus on cultivation under stress conditions**, *Biotechnol. Adv.*, 31 (2013), pp. 1532–1542.
- [5] S. Dickinson, M. Mientus, D. Frey, A. Amini-Hajibashi, S. Ozturk, F. Shaikh, D. Sengupta, M. M. El-Halwagi, **A review of biodiesel production from microalgae**, *Clean Technol. Environ. Policy*, 19 (2017), pp. 637–668.
- [6] S. Khanra, M. Mondal, G. Halder, O. N. Tiwari, K. Gayen, T. K. Bhowmick, **Downstream processing of microalgae for pigments, protein and carbohydrate in industrial application: A review**, *Food Bioprod. Process.*, 110 (2018), pp. 60–84.
- [7] Y. Shen, W. Yuan, Z. J. Pei, Q. Wu, E. Mao, **Microalgae mass production methods**, *Trans. ASABE*, 52 (2009), pp. 1275–1287.
- [8] M. Huntley, Z. Johnson, S. Brown, D. Sills, L. Gerber, I. Archibald, S. Machesky, J. Granados, C. H. Greene, **Demonstrated large-scale production of marine microalgae for fuels and feed**, *Algal Res.-Biomass Biofuels Bioprod.*, 10 (2015), p. 249.

- [9] E. Jankowska, A. K. Sahu, P. Oleskowicz-Popiel, **Biogas from microalgae: review on microalgae's cultivation, harvesting and pretreatment for anaerobic digestion**, *Renew. Sustain. Energy Rev.*, 75 (2017), pp. 692–709.
- [10] N. D. Lourenço, J. A. Lopes, C. F. Almeida, M. C. Sarraguça, H. M. Pinheiro, **Bioreactor monitoring with spectroscopy and chemometrics: a review**, *Anal. Bioanal. Chem.*, 404 (2012), pp. 1211–1237.
- [11] G. Rao, A. Moreira, K. Brorson, **Disposable bioprocessing: the future has arrived**, *Biotechnol. Bioeng.*, 102 (2009), pp. 348–356.
- [12] P. Harms, Y. Kostov, G. Rao, **Bioprocess monitoring**, *Curr. Opin. Biotechnol.*, 13 (2002), pp. 124–127.
- [13] D. G. Spiller, C. D. Wood, D. A. Rand, M. R. H. White, **Measurement of single-cell dynamics**, *Nature*, 465 (2010), pp. 736–745.
- [14] C. Komives, R. S. Parker, **Bioreactor state estimation and control**, *Curr. Opin. Biotechnol.*, 14 (2003), pp. 468–474.
- [15] H. T. D. Nguyen, A. Ramli, L. M. Kee, **A review on methods used in analysis of microalgae lipid composition**, *J. Jpn. Inst. Energy*, 96 (2017), pp. 532–537.
- [16] S. Beutel, S. Henkel, **In situ sensor techniques in modern bioprocess monitoring**, *Appl. Microbiol. Biotechnol.*, 91 (2011), p. 1493.
- [17] J. Claßen, F. Aupert, K. F. Reardon, D. Solle, T. Scheper, **Spectroscopic sensors for in-line bioprocess monitoring in research and pharmaceutical industrial application**, *Anal. Bioanal. Chem.*, 409 (2017), pp. 651–666.
- [18] H. Wagner, Z. Liu, U. Langner, K. Stehfest, C. Wilhelm, **The use of FTIR spectroscopy to assess quantitative changes in the biochemical composition of microalgae**, *J. Biophotonics*, 3 (2010), pp. 557–566.

- [19] S. André, L. S. Cristau, S. Gaillard, O. Devos, É. Calvosa, L. Duponchel, **In-line and real-time prediction of recombinant antibody titer by in situ Raman spectroscopy**, *Anal. Chim. Acta*, 892 (2015), pp. 148–152.
- [20] S. M. Faassen, B. Hitzmann, **Fluorescence spectroscopy and chemometric modeling for bioprocess monitoring**, *Sensors*, 15 (2015), pp. 10271–10291.
- [21] B. R. Wood, P. Heraud, S. Stojkovic, D. Morrison, J. Beardall, D. McNaughton, **A portable Raman acoustic levitation spectroscopic system for the identification and environmental monitoring of algal cells**, *Anal. Chem.*, 77 (2005), pp. 4955–4961.
- [22] P. Heraud, J. Beardall, D. McNaughton, B. R. Wood., **In vivo prediction of the nutrient status of individual microalgal cells using Raman microspectroscopy**, *FEMS Microbiol. Lett.*, 275 (2007), pp. 24–30.
- [23] H. J. Butler, L. Ashton, B. Bird, G. Cinque, K. Curtis, J. Dorney, K. Esmonde-White, N. J. Fullwood, B. Gardner, P. L. Martin-Hirsch, M. J. Walsh, M. R. McAinsh, N. Stone, F. L. Martin, **Using Raman spectroscopy to characterize biological materials**, *Nat. Protoc.*, 11 (2016), pp. 664–687.
- [24] M. Podevin, I. A. Fotidis, I. Angelidaki, **Microalgal process-monitoring based on high-selectivity spectroscopy tools: status and future perspectives**, *Crit. Rev. Biotechnol.*, 38 (2018), pp. 704–718.
- [25] A. M. Herrero, **Raman spectroscopy for monitoring protein structure in muscle food systems**, *Crit. Rev. Food Sci. Nutr.*, 48 (2008), pp. 512–523.
- [26] T.-H. Lee, J.-S. Chang, H.-Y. Wang, **Rapid and in vivo quantification of cellular lipids in *Chlorella vulgaris* using Near-Infrared Raman spectrometry**, *Anal. chem.*, 85 (2013), pp. 2155-2160.

- [27] X. Wei, D. Jie, J. J. Cuello, D. J. Johnson, Z. Qiu, Y. He, **Microalgal detection by Raman microspectroscopy**, *Trac-Trends Anal. Chem.*, 53 (2014), pp. 33–40.
- [28] H. Wu, J. V. Volponi, A. E. Oliver, A. N. Parikh, B. A. Simmons, S. Singh, **In vivo lipidomics using single-cell Raman spectroscopy**, *Proc. Natl. Acad. Sci.*, 108 (2011), pp. 3809–3814.
- [29] S. K. Sharma, D. R. Nelson, R. Abdrabu, B. Khraiwesh, K. Jijakli, M. Arnoux, M. J. O'Connor, T. Bahmani, H. Cai, S. Khapli, R. Jagannathan, K. Salehi-Ashtiani, **An integrative Raman microscopy-based workflow for rapid in situ analysis of microalgal lipid bodies**, *Biotechnol. Biofuels*, 8 (2015), p. 164.
- [30] A. N. Ramya, P. S. Ambily, B. S. Sujitha, M. Arumugam, K. K. Maiti, **Single cell lipid profiling of *Scenedesmus quadricauda* CASA-CC202 under nitrogen starved condition by surface enhanced Raman scattering (SERS) fingerprinting**, *Algal Res.*, 25 (2017), pp. 200–206.
- [31] T. Wang, Y. Ji, Y. Wang, J. Jia, J. Li, S. Huang, D. Han, Q. Hu, W. E. Huang, J. Xu, **Quantitative dynamics of triacylglycerol accumulation in microalgae populations at single-cell resolution revealed by Raman microspectroscopy**, *Biotechnol. Biofuels*, 7 (2014), p. 58.
- [32] Y. Ji, Y. He, Y. Cui, T. Wang, Y. Wang, Y. Li, W. E. Huang, J. Xu, **Raman spectroscopy provides a rapid, non-invasive method for quantitation of starch in live, unicellular microalgae**, *Biotechnol. J.*, 9 (2014), pp. 1512–1518.
- [33] S. He, S. Fang, W. Xie, P. Zhang, Z. Li, D. Zhou, Z. Zhang, J. Guo, C. Du, J. Du, D. Wang, **Assessment of physiological responses and growth phases of different microalgae under environmental changes by Raman spectroscopy with chemometrics**, *Spectrochim. Acta. A. Mol. Biomol. Spectrosc.*, 204 (2018), pp. 287–294.

- [34] J. Rüger, N. Unger, I. W. Schie, E. Brunner, J. Popp, C. Krafft, **Assessment of growth phases of the diatom *Ditylum brightwellii* by FT-IR and Raman spectroscopy**, *Algal Res.*, 19 (2016), pp. 246–252.
- [35] M. S. Parker, T. Mock, E. V. Armbrust, **Genomic insights into marine microalgae**, *Annu. Rev. Genet.*, 42 (2008), pp. 619–645.
- [36] R. J. W. Brooijmans, R. J. Siezen, **Genomics of microalgae, fuel for the future?**, *Microb. Biotechnol.*, 3 (2010), pp. 514–522.
- [37] T. Chen, Q. Zhao, L. Wang, Y. Xu, W. Wei, **Comparative metabolomic analysis of the green microalga *Chlorella sorokiniana* cultivated in the single culture and a consortium with bacteria for wastewater remediation**, *Appl. Biochem. Biotechnol.*, 183 (2017), pp. 1062–1075.
- [38] R. Willamme, Z. Alsafera, R. Arumugam, G. Eppe, F. Remacle, R. D. Levine, C. Remacle, **Metabolomic analysis of the green microalga *Chlamydomonas reinhardtii* cultivated under day/night conditions**, *J. Biotechnol.*, 215 (2015), pp. 20–26.
- [39] E. da Costa, J. Silva, S. H. Mendonça, M. H. Abreu, M. R. Domingues, **Lipidomic approaches towards deciphering glycolipids from microalgae as a reservoir of bioactive lipids**, *Mar. Drugs*, 14 (2016), p. 101.
- [40] E. K. Matich, M. Ghafari, E. Camgoz, E. Caliskan, B. A. Pfeifer, B. Z. Haznedaroglu, G. E. Atilla-Gokcumen, **Time-series lipidomic analysis of the oleaginous green microalga species *Ettlia oleoabundans* under nutrient stress**, *Biotechnol. Biofuels*, 11 (2018), p. 29.
- [41] R. Puzanskiy, E. Tarakhovskaya, A. Shavarda, M. Shishova, **Metabolomic and physiological changes of *Chlamydomonas reinhardtii* (Chlorophyceae,**

- Chlorophyta) during batch culture development**, J. Appl. Phycol., 30 (2018), pp. 803–818.
- [42] H. Lv, G. Qu, X. Qi, L. Lu, C. Tian, Y. Ma, **Transcriptome analysis of *Chlamydomonas reinhardtii* during the process of lipid accumulation**, Genomics, 101 (2013), pp. 229–237.
- [43] F. Hadj-Romdhane, P. Jaouen, J. Pruvost, D. Grizeau, G. Van Vooren, P. Bourseau, **Development and validation of a minimal growth medium for recycling *Chlorella vulgaris* culture**, Bioresour. Technol., 123 (2012), pp. 366–374.
- [44] S. H. Hutner, L. Provasoli, A. Schätz, C. P. Haskins, **Some approaches to the study of the role of metals in the metabolism of microorganisms**, Proc. Am. Phil. Soc., 94 (1950), pp. 152-170.
- [45] M. P. Caporgno, A. Taleb, M. Olkiewicz, J. Font, J. Pruvost, J. Legrand, C. Bengoa, **Microalgae cultivation in urban wastewater: Nutrient removal and biomass production for biodiesel and methane**, Algal Res., 10 (2015), pp. 232–239.
- [46] R. Michalski, I. Kurzyca, **Determination of nitrogen species (nitrate, nitrite and ammonia ions) in environmental samples by ion chromatography**, Pol. J. Environ. Stud., 15 (2006), pp. 5–18.
- [47] M. D. Macias-Sanchez, C. Mantell, M. Rodriguez, E. Martinez de la Ossa, L. M. Lubian, O. Montero, **Supercritical fluid extraction of carotenoids and chlorophyll a from *Nannochloropsis gaditana***, J. Food Eng., 66 (2005), pp. 245-251.
- [48] R. J. Ritchie, **Consistent sets of spectrophotometric chlorophyll equations for acetone, methanol and ethanol solvents**, Photosynth. Res., 89 (2006), pp. 27–41.
- [49] H. Zhang, Z. Gao, Z. Li, H. Du, B. Lin, M. Cui, Y. Yin, F. Lei, C. Yu, C. Meng, H. Zhang, Z. Gao, Z. Li, H. Du, B. Lin, M. Cui, Y. Yin, F. Lei, C. Yu, C. Meng, **Laser Radiation**

Induces Growth and Lipid Accumulation in the Seawater Microalga *Chlorella pacifica*, *Energies*, 10 (2017), p. 1671.

- [50] A. Assaf, C. B. Y. Cordella, G. Thouand, **Raman spectroscopy applied to the horizontal methods ISO 6579:2002 to identify *Salmonella* spp. in the food industry**, *Anal. Bioanal. Chem.*, 406 (2014), pp. 4899–4910.
- [51] C. B. Y. Cordella, D. Bertrand, **SAISIR: A new general chemometric toolbox**, *TrAC Trends Anal. Chem.*, 54 (2014), pp. 75–82.
- [52] F. Dieterle, A. Ross, G. Schlotterbeck, H. Senn, **Probabilistic quotient normalization as robust method to account for dilution of complex biological mixtures. Application in 1H NMR metabonomics**, *Anal. Chem.*, 78 (2006), pp. 4281–4290.
- [53] Q. Kong, L. Li, B. Martinez, P. Chen, R. Ruan, **Culture of microalgae *Chlamydomonas reinhardtii* in wastewater for biomass feedstock production**, *Appl. Biochem. Biotechnol.*, 160 (2009), p. 9.
- [54] G. Van Vooren, F. Le Grand, J. Legrand, S. Cuiné, G. Peltier, J. Pruvost, **Investigation of fatty acids accumulation in *Nannochloropsis oculata* for biodiesel application**, *Bioresour. Technol.*, 124 (2012), pp. 421–432.
- [55] S. Friedrich, E. Spukerman, **Chlorophyll a Fluorescence and Absorption in Two *Chlamydomonas* Species**, *Ecol. Chem. Eng. A*, 16 (2009), pp. 1501–1513.
- [56] Y. Y. Hsu, M. C. Chen, K. E. Lim, C. Chang, **Reproducibility of hippocampal single-Voxel proton MR spectroscopy and chemical shift imaging**, *AJR Am. J. Roentgenol.*, 176 (2001), pp. 529–536.
- [57] O. Samek, A. Jonas, Z. Pilat, P. Zemanek, L. Nedbal, J. Triska, P. Kotas, M. Trtilek, **Raman Spectroscopy for the characterization of algal cells**, *Proc. of SPIE*, 7746 (2010), p. 77460.

- [58] N. D. T. Parab, V. Tomar, **Raman Spectroscopy of Algae: A Review**, J. Nanomedicine Nanotechnol., 3 (2012), pp. 131-137.
- [59] De Gelder Joke, De Gussem Kris, Vandenabeele Peter, Moens Luc, **Reference database of Raman spectra of biological molecules**, J. Raman Spectrosc., 38 (2007), pp. 1133–1147.
- [60] A. S. Mostaert, C. Giordani, R. Crockett, U. Karsten, R. Schumann, S. P. Jarvis, **Characterisation of amyloid nanostructures in the natural adhesive of unicellular subaerial algae**, J. Adhes., 85 (2009), pp. 465–483.
- [61] D. Garfinkel, **Raman Spectra of Amino Acids and Related Compounds. XII. Various Amino Acids Derived from Proteins and Creatine 1,2**, J. Am. Chem. Soc., 80 (1958), pp. 3827–3831.
- [62] T. Lien, G. Knutsen, **Synchronous growth of *Chlamydomonas reinhardtii* (chlorophyceae): a review of optimal conditions**, J. Phycol., 15 (2008), pp. 191–200.
- [63] Y. Ren, Y. Ji, L. Teng, H. Zhang, **Using Raman spectroscopy and chemometrics to identify the growth phase of *Lactobacillus casei* Zhang during batch culture at the single-cell level**, Microb. Cell Factories, 16 (2017), p. 233.
- [64] A. Sirikhachornkit, A. Suttangkakul, S. Vuttipongchaikij, P. Juntawong, **De novo transcriptome analysis and gene expression profiling of an oleaginous microalga *Scenedesmus acutus* TISTR8540 during nitrogen deprivation-induced lipid accumulation**, Sci Rep., 8 (2018), p. 3668.
- [65] Y. Yao, Y. Lu, K.-T. Peng, T. Huang, Y.-F. Niu, W.-H. Xie, W.-D. Yang, J.-S. Liu, H.-Y. Li, **Glycerol and neutral lipid production in the oleaginous marine diatom *Phaeodactylum tricornutum* promoted by overexpression of glycerol-3-phosphate dehydrogenase**, Biotechnol. Biofuels, 7 (2014), p. 110.

Supplementary data

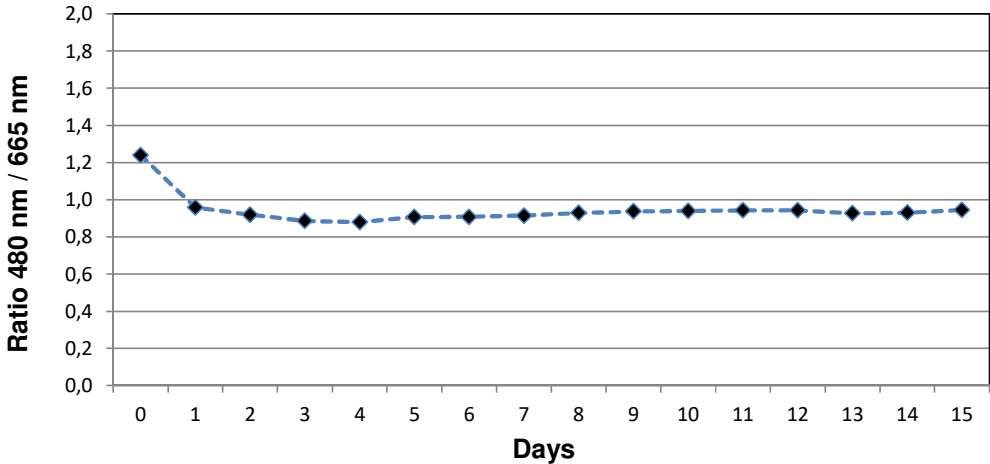


Fig. 1. Ratio of optical density 480 nm (beta-carotene) to 665 nm (chlorophyll a).

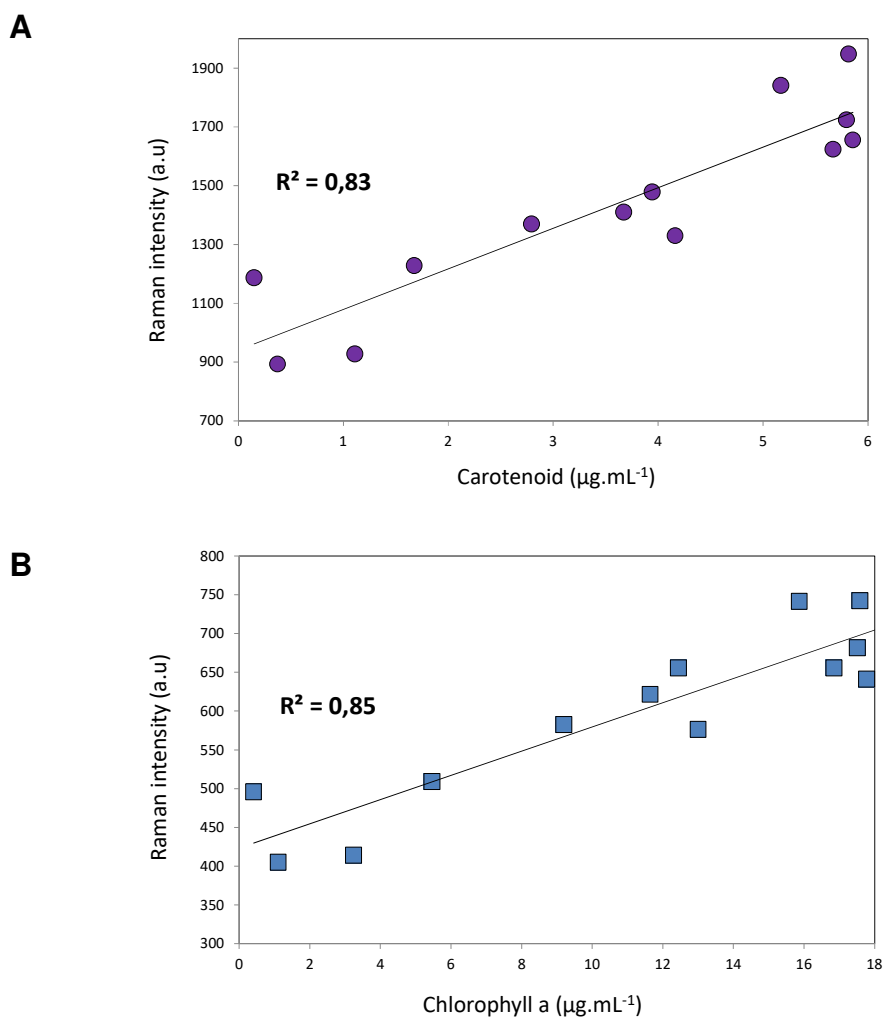


Fig.2. A. Correlation of the Raman band intensity at 1523 cm^{-1} with the beta-carotene dosage from the growth of *Chlamydomonas reinhardtii* in photobioreactors ($R^2 = 0.83$). Days of growth from 0 to 12 are represented for graphic visualization **B.** Correlation of the Raman band at 1325 cm^{-1} with the chlorophyll a dosage from the growth of *Chlamydomonas reinhardtii* in photobioreactors ($R^2 = 0.85$). Days of growth from 0 to 12 are represented for graphic visualization.